Robotica: (2021) volume 39, pp. 42–54. © The Author(s) 2020. Published by Cambridge University Press
doi:10.1017/S0263574720000156

Stability Improvement of Segway Based on Tire Model Using the SEA

Haneul Yun, Hongyu Zhang and Jangmyung Lee*

Pusan National University

(Accepted February 4, 2020. First published online: February 28, 2020)

SUMMARY
This study proposes the use of a series elastic actuator (SEA) in a Segway to improve the stability of the tires during linear and curved driving, thus improving the comfort of the driver and ensuring driving stability. Recently, Segway has been developed continuously for intelligent mobile vehicles and the performance of Segway is being enhanced. Therefore, safety factors during the Segway driving have been considered seriously. In most of the developments and studies on Segway, the optimization and improvement of the controller component have been tackled and there are few studies on the safety devices and the stability of driving. The impact and vibration generated from the ground due to uneven road surfaces considerably influence the force exerted on the tire, which further affects driving stability. This research focuses on the control of the SEA based on the tire model to improve the driving stability of Segway. The performance of the proposed algorithm to improve the stability of the driver has been verified by straight and curved paths driving experiments with the tire model.

KEYWORDS: Series elastic actuator (SEA); Tire model; Segway; Stability improvement.

1. Introduction

The latest developments in industrial technology, lifestyle changes, and improvements in the standard of living have changed the modes of transport systems; they have been especially affected by the rapid development of controllers, batteries, and materials technology. So, the demands of development for personal transport systems are constantly increasing and they had been developed constantly for 20 years. In the field of personal mobilities, the Segway, invented by American inventor Dean Kamen in 2001, has a different structure and different modes of operation compared to existing transport systems. Since the Segway is light and portable, it can be used as a substitute for a short distance moving transport like the bicycle or motorcycle. Since its inception, the Segway has attracted the attention of many researchers and has been studied by many people.[1–4] From a practical perspective, widespread usage of the Segway depends on its control stability and driving safety. The Segway possesses a very evident disadvantage in its lack of battery capacity and safety when driven over long distances. Despite these disadvantages, most of the research on personal mobility has focused on optimization strategies to achieve superior performance, and optimum design of the controllers. There are only a few studies on safety and stability problems, such as accident prevention and curve driving.[5–8] If the Segway turns at a high speed, the centripetal force will change in an instant; this change will generate a huge lateral force on the tire that leads to increase in the risk of rollover. In addition, when the road surface is uneven, the unexpected external force and vibration generated from impact with the ground influence the forces acting on the tire considerably. The uneven force acting on the tire and the instantaneously large impact force will greatly affect the vehicle, giving rise to an instability of its body, that in turn will correspondingly increase the risk of rollover.

* Corresponding author. E-mail: jmlee@pusan.ac.kr

https://doi.org/10.1017/S0263574720000156 Published online by Cambridge University Press

Table I. List of the main parameters.

V_x	**Longitudinal velocity**	F_m	**Force generated by the motor**
V_y	Lateral velocity	M_m	Mass of the motor
F_x	Longitudinal force	M_b	Mass of the ball screw
F_y	Lateral force	K_s	Constant of the spring
F_z	Vertical force to the tire	b_m	Damping ratios of the motor
λ	Slip ratio	b_l	Damping ratios of the load
α	Side slip angle	F_l	Output force of the load end
r	Radius of gyration	F_{ext}	External force
ω_y	Angular velocity of the tire	F_G	Gravity force at the center of mass
R	Radius of rotation	F_{CP}	Centripetal force
L	Distance of left and right tires	F_F	Vertical force to the footplate
V_L	Velocity of the left tire	V_{Segway}	Velocity of the Segway
V_R	Velocity of the right tire	F_{Segway}	Gravity force of the Segway
		F_d	Compensating force

Therefore, in this study, the series elastic actuator (SEA) was used to construct a suspension system that will be installed within the Segway model to improve the stability of linear and curved driving. During linear motion, the longitudinal forces that propel the Segway will be adversely affected by external forces. The SEA will reduce the disturbances acting on these longitudinal forces. The height of the SEA changes according to the external force generated during the linear motion. Also, if external force acting on the Segway is small like as vibrations, external force can be cancelled because the springs of the SEA can be operated like a low-pass filter.[9] When turning, the lateral forces on the left and right tires will act on them differently.[10–13] The Segway will easily rollover when the difference in lateral forces acting on the left and right tires is very large.[14–17] In this case, the SEA adjusts the height of the footplate attached above the Segway so that these lateral forces are similar in magnitude. The height of the SEA changes according to the centripetal force generated during the turn, so that the center of gravity of the driver is shifted to a safer point; this shift in the center of gravity reduces the difference between the lateral forces on the left and right tires, ensuring a balanced load on the tires. A balanced load reduces the probability of vehicle rollover caused by the unequal forces on the two tires, thereby, achieving guaranteed safety and stability while the vehicle is turning. Therefore, the function the SEA is to generate a compensating force that corresponds to the measured external force applied on the Segway; this compensating force stabilizes the tires. Notice that the force acting on the tires of Segway that is caused by impact from uneven road surfaces or inertia force is neutralized by the compensation. Thus, the SEA can be used as a low-cost high-performance active suspension system.[18–20]

In this work, we propose to use the SEA to form an active suspension system and improve vehicle stability and driver comfort. This work contributes to current research by applying the SEA to compensate for the force of impact on the tires owing to uneven road surfaces or other reasons. The advantage of the SEA in neutralizing the effects of tire impact is demonstrated by comparing its performance with that of a personal mobility device that is known to possess state-of-the-art stability and driver comfort. The actual road test proves that the vehicles having the proposed active suspension system with SEA devices installed are more stable than the vehicles without such a suspension system. This paper consists of five sections. Section 1 is the introduction; Section 2 describes the establishment and construction of the tire model; Section 3 discusses the structure of the series of elastic brakes and design of the SEA; Section 4 analyzes the motion of the Segway; and Section 5 discusses the experiment and its result. The conclusions drawn from this study and future research will be presented in the last section. To avoid any confusion, also, the list of parameters used in this research has been summarized in Table I.

2. Modeling of the Tire

Because of the interaction between the tire and ground, the vehicle produces various types of movements. The characteristics of the tire play an important role in these motions. The lateral force characteristic of the tire is the basis of the stability of the vehicle. The nonlinear characteristics of the tire and the steering characteristics of the vehicle have a high influence on its driving stability.[10] The

https://doi.org/10.1017/S0263574720000156 Published online by Cambridge University Press

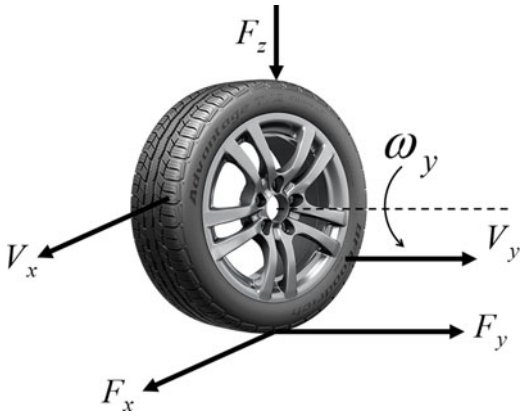


Fig. 1. Tire model diagram in the SAE for the force analysis.

stability of the vehicle's handling depends to a large extent on the lateral deflection characteristics of the tire; these are determined by the relationships among the various vertical and lateral forces acting on the lower regions of the tire, by the longitudinal forces, side angles, and the longitudinal slip ratio. Therefore, establishing an accurate tire dynamics model is the basis for simulation studies on the stability of the vehicle while it is in motion.

The tire model is divided into three categories: the theoretical, empirical, and adaptive models. At present, the most popular tire models in the world are Taehyun analysis tire model,[11] "Magic Formula" tire experience model,[12–14] unification Exponential radius tire model,[15] neural network adaptive computer tire model,[16,17] and a few others. Among the most popular tire models, the HB Pacejka tire model was proposed by Professor HB Pacejka of Del Polytechnic University in the Netherlands in 1987. It was later renamed the Magic Formula tire model. This is an empirical tire model obtained by fitting the experimental data. The experiments are carried out using a special test bench or test vehicle, which can eliminate secondary factors and simulate the driving conditions necessary to accurately reproduce the various working environments of the tire. The instrument used to detect various types of data during the test has high precision and sensitivity and is equipped with a powerful data processing system to ensure accurate and reliable test data collection and analysis. The HB Pacejka tire model can use a set of formulas to fully express the mechanical properties of the tire under true working conditions, so it is called the "Magic Formula". Owing to its precision and concision, it is broadly applied in the research of moving vehicle dynamics. In today's tire characterizations, the magic formula is increasingly dominant, for its high fitting precision, its applicability within a certain range beyond the limit value, and the high degree of trust and confidence placed in it. It is suitable for the theoretical and predictive analysis of automotive dynamics. Therefore, this study uses the Pacejka tire model to analyze the specific tire characteristics. The tire model in Magic Formula uses the Society of Automotive Engineers model, and the tire model for the force analysis is shown in Fig. 1.

The calculation of tire forces uses the Magic Formula to establish the relationship between the input and output variables. Figure 2 illustrates the relationship of Magic Formula between the input and output variables.

In Fig. 2, the λ represents the slip ratio between the tire and the ground when the Segway runs straight or curved paths. The α represents the side slip angle which is the difference between the target direction of the tire and its real motion vector. The side slip angle 0 indicates that the tire is going straightforward without the side slip. A typical peak slip angle for tire is around 3–6°. The slip ratio λ and the side slip angle α can be calculated as follows:

$$\lambda = V_{\text{Segway}} - \omega_y r / V_{\text{Segway}} \tag{1}$$

$$\alpha = \arctan\left(V_x / V_y\right) \tag{2}$$

The basic form of equation about the Magic Formula tire model is shown as follows:

$$F = D \sin\{C \arctan[B(X + S_h) - E(B(X + S_h) - \arctan B(X + S_h))]\} + S_v \tag{3}$$

https://doi.org/10.1017/S0263574720000156 Published online by Cambridge University Press

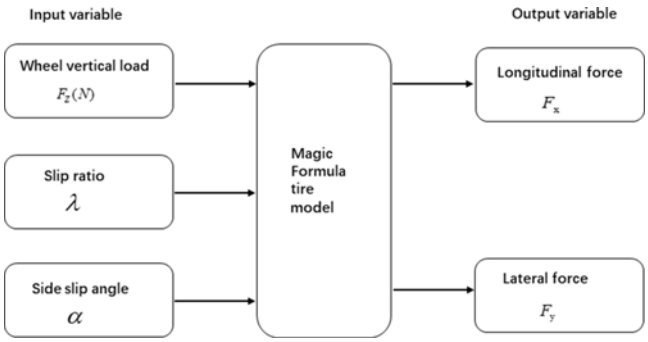


Fig. 2. Diagram of input–output relationships in Magic Formula.

where F (F_x or F_y) represents the force acting on the tires, D is the peak factor, C is the shape factor, B is the stiffness factor, and E is the curvature factor. X represents the side slip angle α or the slip ratio λ for computing lateral or longitudinal force, respectively. The coefficients B, C, D, and E are calculated from additional equations and the coefficients found in the tire data. S_h and S_v represent the horizontal drift and the vertical drift, respectively. Using Eq. (3), the lateral and the longitudinal force acting on the tires can be obtained. The diverse coefficients (B, C, D, and E) can be obtained using the experimental data in the fitting computation.

2.1. Longitudinal force of the steady-state braking environment

The slip ratio (λ) has a direct influence on the angular speed of the tire while the vehicle is in motion. Furthermore, the angular speed changes under the same driving force or brake force. In general case, Eq. (3) is used to calculate the longitudinal force acting on the tires. But the horizontal and the vertical drifts are not generated because the Segway consists of two tires without the camber. So, S_h and S_v in Eq (3) can be eliminated. In order to calculate the longitudinal force, also, F and X in Eq. (3) are substituted for F_x and λ, respectively. So, the relationships between the longitudinal force F_x, vertical load F_z, and slip ratio λ are expressed as follows:

$$F_x = D_x \sin\{C_x \arctan[B_x\lambda - E_x(B_x\lambda - \arctan B_x\lambda)]\} \tag{4}$$

where $D_x = a_1F_z^2 + a_2F_z$, $C_x = 1.65$, $B_x = B_xC_xD_x/C_xD_x$, $E_x = a_6F_z^2 + a_7F_z + a_8$, $B_xC_xD_x = a_3 \sin[a_4 \arctan(a_5F_z)]$, and $a_1, a_2, \cdots, a_8$ are the fitting parameters to calculate the longitudinal force.

2.2. Lateral force of the steady-state steering environment

In order to calculate the lateral force, S_h and S_v can be eliminated and F and X in Eq. (3) are substituted for F_y and α, respectively. So, the relationships between lateral force F_y, side slip angle α, and vertical load F_z are shown as follows:

$$F_y = D_y \sin\left\{C_y \arctan\left[B_y\alpha - E_y\left(B_y\alpha - \arctan B_y\alpha\right)\right]\right\} \tag{5}$$

where $D_y = b_1F_z^2 + b_2F_z$, $C_y = 1.3$, $B_y = B_yC_yD_y/C_yD_y$, $E_y = b_6F_z^2 + b_7F_z + b_8$, $B_yC_yD_y = b_3 \sin[b_4 \arctan(b_5F_z)]$, and $b_1, b_2, \cdots, b_8$ are the fitting parameters to calculate the lateral force.

2.3. Simultaneous steering and braking

The solution of Eqs. (4) and (5) will yield the tire force for a single variable condition, which turns out the relations among different tire forces in the combined condition of turning and breaking are as follows:

$$^{C}F_x = \frac{\sigma_x}{\sigma}F_x, \; ^{C}F_y = \frac{\sigma_y}{\sigma}F_y \tag{6}$$

where the longitudinal and lateral forces in combined condition are $^{C}F_x$ and $^{C}F_y$, respectively, $\sigma = \sqrt{\sigma_x{}^2 + \sigma_y{}^2}$, $\sigma_x = -\frac{\lambda}{1+\lambda}$, and $\sigma_y = -\frac{\tan\alpha}{1+\lambda}$. The above Eqs. (4)–(6) are a mathematical description of the tire mode, while the overall dynamic model of the tire for MATLAB simulation is shown in Fig. 3.

https://doi.org/10.1017/S0263574720000156 Published online by Cambridge University Press

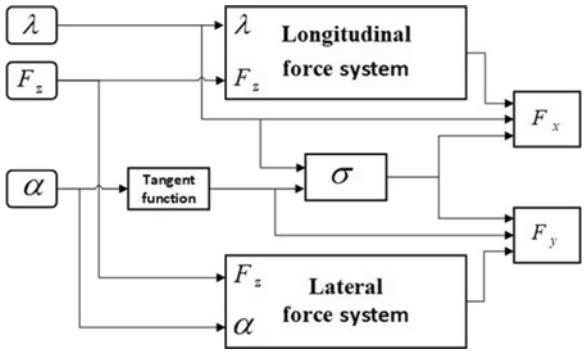


Fig. 3. Overall block diagram of Magic Formula tire model.

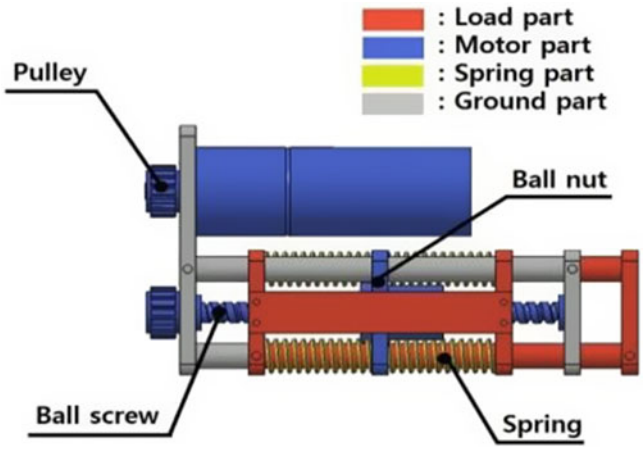


Fig. 4. CAD design of the SEA model.

This model consists of three inputs (F_z, λ, α) and two outputs (F_x, F_y). The three data are used to calculate the longitudinal and lateral force. Three input data are passing through the longitudinal and lateral force systems. The F_z and λ are used for the inputs of the longitudinal force system. F_z and α are used for the inputs of the lateral force system.

3. Design and Control of SEA

In 1995, Gill A. Pratt and Matthew M. Williamson proposed a model called SEA,[9] which is an actuator that combines elastic elements with conventional actuators. A spring is placed between the motor and end of an actuator. Owing to this structure, the SEA has a robust characteristic to external influence. When the road surface is uneven or the vehicle takes high-speed runs, the impact force on the tires will be transmitted to the driver through the vehicle body. At the same time, the driver will apply an impact force on the end of an actuator; the spring, however, can absorb a part of the impact, which will stabilize the longitudinal and lateral forces on the tire and make the vehicle more stable. Also, when the vehicle turns at high-speed, the lateral forces acting on the tires are increased. When the lateral force is increased over the critical value, the stability of vehicle is reduced at the turning motion and the possibility of rollover is increased. To keep the lateral forces below the critical value, the SEA has been utilized. Notice that the lateral forces can be calculated using the Magic Formula in Eq. (3). If the lateral force acting on one of the two tires exceeds the critical value, the SEA adjusts the Segway to reduce the lateral force. Therefore, this study proposes to add the SEA to the Segway. Because the SEA can easily control the force, it works as an actuator for a high-performance suspension mechanism that can compensate for both a state of unbalanced forces, and neutralize external forces such as the impact force.[18–20]

3.1. Design of the SEA for an active suspension system

In this study, the SEA described in Fig. 4 is proposed to compensate for the external force by using a suspension mechanism.

https://doi.org/10.1017/S0263574720000156 Published online by Cambridge University Press

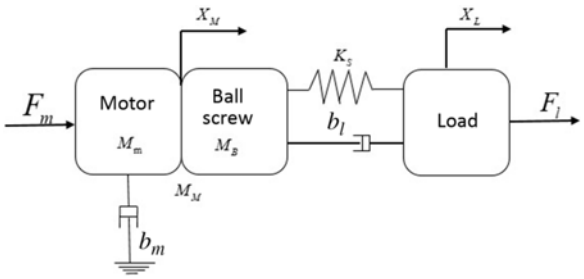


Fig. 5. Dynamic model of the SEA and its translational motions.

The SEA of Fig. 4 consists of a DC motor, pair of pulleys, a ball screw and nut, a set of linear springs, and load end part. The rotational movement of the motor shaft is transmitted to the ball screw and then converted into a linear movement of the load part by the ball screw. A pair of linear springs are mounted on between the ball screw nut and load part, and the force generated by the motor is transmitted to the end of the load part. The SEA can be used as a suspension because it can measure the external force by using the compression length of the spring and generates a reaction force in the opposite direction acting on the external force.

3.2. Modeling of the SEA

Because the SEA converts the rotational motion of the motor into linear motion through the ball screw, the equivalent model of the SEA can be composed of a translational motion system. The SEA equivalent model of translational motion is shown in Fig. 5.

In this dynamic model, the force F_m is generated by the motor, where M_m and M_b are the mass of the motor and ball screw, respectively. Because the motor and ball screw move together through the timing belt, they can be seen as a whole. So, M_M comprises the mass of the motor and ball screw; K_s is the constant of the spring; finally, b_m and b_l are the damping ratios of the motor and load, respectively. F_l is the output force of the load end, as shown in Fig. 5. The SEA is essentially a flexible system consisting of two masses, and its dynamics are analyzed using a two-mass dynamic model.[21] The SEA can be modeled as a combination of the three free bodies dynamics: motors, springs, and load systems. The dynamic equations of the three systems can be expressed as follows:

$$M_M\ddot{X}_M + b_{\mathrm{m}}\ddot{X}_M = F_{\mathrm{m}} + F_{\mathrm{l}} \tag{7}$$

$$K_s\,(X_M - X_L) = F_{\mathrm{l}} \tag{8}$$

$$M_L\ddot{X}_L + b_{\mathrm{l}}\ddot{X}_L = F_{\mathrm{l}} - F_{ext} \tag{9}$$

where F_m is the force generated by the motor, F_l is the force generated by the deformation of the spring. F_{ext} is an external force applied to the SEA from the outside, which is generated between tires and the road. Each system can be alternatively expressed by the Laplace transformation as follows:

$$P_{\mathrm{m}}(s) = \frac{\mathbf{1}}{M_M s^2 + b_M s} \tag{10}$$

$$P_{\mathrm{s}}(s) = \frac{\mathbf{1}}{K_s} \tag{11}$$

$$P_{\mathrm{l}}(s) = \frac{\mathbf{1}}{M_{\mathrm{l}} s^2 + b_l s}. \tag{12}$$

The above section describes the SEA; next, we will discuss the motion of Segway.

4. Segway Motion

It is well known that the lateral and longitudinal forces on the tires are generated when Segway is running straight and turning, respectively. The forces acting on the tires are mainly influenced by

https://doi.org/10.1017/S0263574720000156 Published online by Cambridge University Press



Fig. 6. Segway equipped with the SEA.

external force, inertia force, and centripetal force. If these external forces are very large, forces acting on the tires increase over the critical value. The Segway can be unstable to be rolled over, which may hurt the passenger. The SEA can adjust the left and right footplate of the Segway independently to relieve the unexpected external forces acting on the tires. In order to keep the lateral force or longitudinal force below the critical value, the SEA has been utilized. These forces acting on the tires are always calculated to check whether or not the forces exceed the critical value using the Magic Formula equation. So, in order to keep the lateral force or longitudinal force below the critical value, the SEA has been utilized. Four SEAs are installed at each corner of the Segway footplate as shown in Fig. 6 to adjust the height of each corner of the footplate.

The Segway's driving mode consists of four driving modes, and it includes linear and steering motion as shown in Fig. 7. Linear and steering motion is determined by the radius of rotation, R, and the radius of rotation, R, can be obtained as follows:

$$R = \frac{L\,(V_R + V_L)}{\mathbf{2}\,|V_R - V_L|}. \tag{13}$$

When the speed of the left tire is equal to that of the right tire, the rotational radius is infinity. Otherwise, the rotation radius is greater than zero which causes the vehicle to turn left or right.

In the case of left-turn motion as shown in Fig. 8, the force acting on the footplate is mainly related to the gravity force (F_G) which can be divided into two parts: F_F and F_{CP}. The force F_{CP} is generated by the SEA control to compensate for the centrifugal force and F_F is the vertical force to the footplate. In generating the centripetal force, F_{CP}, the acting point of gravity force on the footplate has been moved to the left, which changes the vertical force F_z to each of the tire. When the vertical force on the tire has been changed, the lateral force of the tires is changed as it is shown in the Magic Formula Eq. (5).

The centrifugal force generated during the turning motion can be compensated by F_{CP} generated with the SEA control as shown in Fig. 8. For the stable left-turn motion of the Segway, the centripetal force and the centrifugal force must be balanced. When the footplate of the Segway is lifted (to the direction of the centripetal force) in order to compensate for the increased centrifugal force, the gravity force is also shifted to the left. The magnitude of centripetal force by this SEA control and centrifugal force by turning motion is the same and their direction is opposite, which can be represented as follows:

$$F_{\text{centripetal}} = -F_{\text{centrifugal}} = \left| \frac{Mv^2}{R} \right| \tag{14}$$

where M is the total mass of the vehicle and its driver, and v is the speed of vehicle.

https://doi.org/10.1017/S0263574720000156 Published online by Cambridge University Press

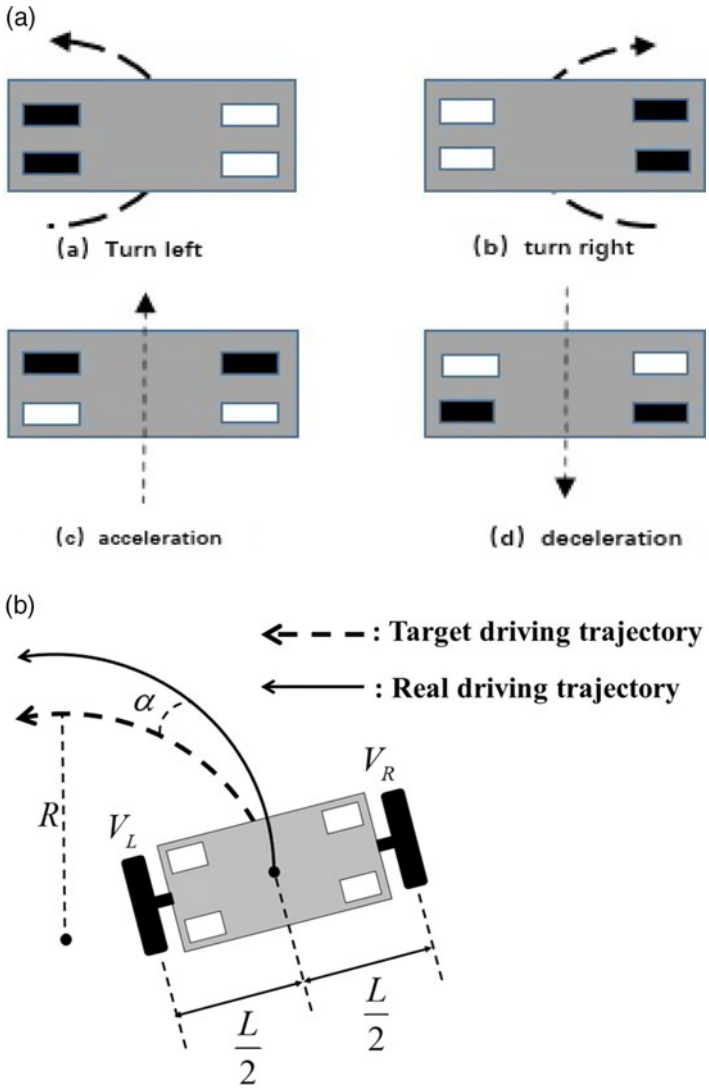


Fig. 7. Four cases of driving motion and related variables for the decision of motion. (a) Four cases of driving mode; (b) left-turn operation.

The load on the tire represented F_z is mainly affected by the weight of the Segway and driver. However, during actual driving, there exist disturbances, F_{ext}, on the tire from the bumpy road surface. Therefore, the total vertical force on the tire, F_z, can be represented as follows:

$$F_Z = F_{\text{Segway}} + F_G + F_{ext} \tag{15}$$

where F_{Segway} represents the gravity force of the Segway body, which is distributed to the left and right tires equally. Notice that F_G is distributed to the left and right wheels unequally as shown in Fig. 8 to compensate for the centrifugal force. The SEA device proposed in this study also compensates for F_{ext}, so that the tire is stable and well-balanced. The unified model that incorporates both the tire and SEA models is shown in Fig. 9.

The value of F_m in Fig. 9 represents the difference between the value of the force measured by the pressure sensor, F_d, and the compensating force produced by the SEA. When the road condition is good, the force of SEA compensation is zero. When the road condition is bumpy, the corresponding force is generated by the SEA device to compensate for the disturbance and to minimize the F_z. When the vehicle turns, footplate of Segway is lifted to compensate the difference of the lateral forces action on the two tires as shown in Fig. 8, and the change in lateral forces caused by increasing centripetal forces is compensated by the SEA, which quickly equalizes the force on the tire. The remaining variables can be measured by the corresponding sensor.

https://doi.org/10.1017/S0263574720000156 Published online by Cambridge University Press

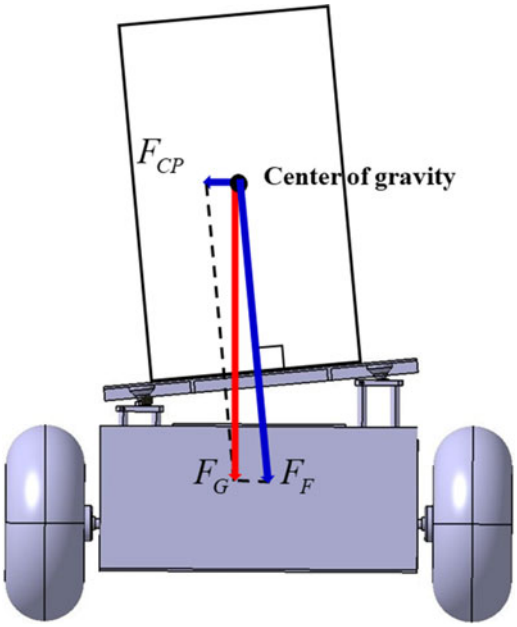


Fig. 8. Compensation of centrifugal force by the SEA control (case of left turn).

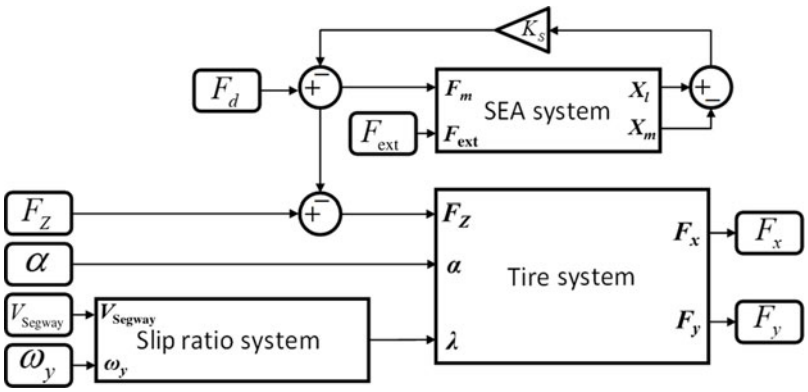


Fig. 9. Block diagram of the entire system.

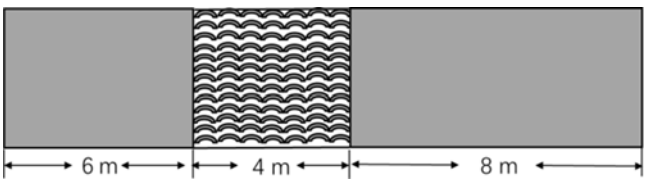


Fig. 10. Illustration of the test-bed for straight line motion experiments.

5. Experiments and Results

In this section, the experiments for linear motion, and high-speed steering motion, with and without the SEA mechanism are carried out. A comparison of the magnitudes of the various fluctuations in force experienced by the tire is carried out to verify the effectiveness of the SEA.

5.1. Experiment in straight line motion

The experiment in straight line motion is carried out on a normal asphalt road with a bumpy area, as shown in Fig. 10.

https://doi.org/10.1017/S0263574720000156 Published online by Cambridge University Press

Table II. Experimental results of straight line motion.

	Left tire	Right tire	Average	External force	Compensated force	Compensation ratio
Without SEA	558.62 N	568.75 N	563.69 N	163.69 N	107.98 N	34%
With SEA	455.17 N	456.25 N	455.71 N	55.71 N		

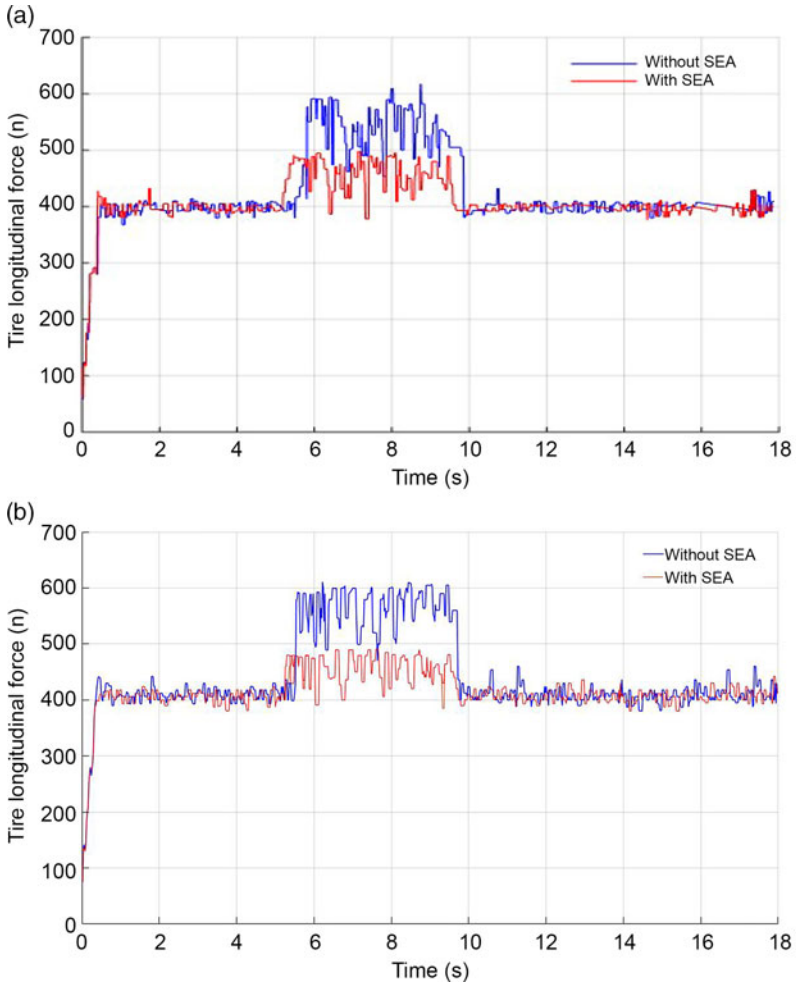


Fig. 11. Longitudinal force of the left and right tire ((a) left tire, (b) right tire).

Under straight line motion conditions, the center of gravity does not shift, and the left and right tires are balanced, making the weight distribution equal between the two tires. Figure 11 shows the experimental result of the longitudinal forces of the left and right tires as an example.

On a normal asphalt road, the road is relatively flat, and the longitudinal forces acting on the two tires are consistently the same, either with or without the SEA equipment (refer to 0–6 and 10–18 s as shown in Fig. 11). During travel on the bumpy area, without the SEA device, the longitudinal force average is about 564 N. In the case of the SEA having been installed, because the SEA compensates for changes in longitudinal forces caused by the external environment, the average longitudinal force is about 456 N. Notice that on the normal asphalt road, the longitudinal force acting on the tires is about 400 N. The external forces caused by the bumpy area are 164 and 56 N without the SEA and with SEA, respectively. Through the above analysis, it is noticed that the SEA device can reduce the instability of Segway by about 34% in case of bumpy area conditions. Note that the abrupt change of the longitudinal force deteriorates the riding comfort of the driver. The longitudinal force acting on the left and right tires, average of longitudinal force acting on two tires, external force caused by the bumpy area, compensated force, and compensation ratio are summarized in Table II.

https://doi.org/10.1017/S0263574720000156 Published online by Cambridge University Press

Table III. Experimental results of rotational motion.

	Lateral force (left tire)	**Lateral force (right tire)**	**Difference of two tires**	**Compensated force**
Without SEA	9.09 N	677.27 N	668.18 N	505.89 N
With SEA	320.45 N	482.72 N	162.29 N	

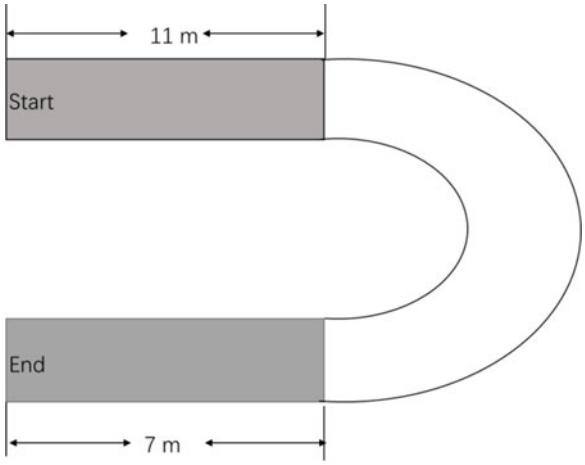


Fig. 12. Illustration of the test-bed for rotational motion experiments.

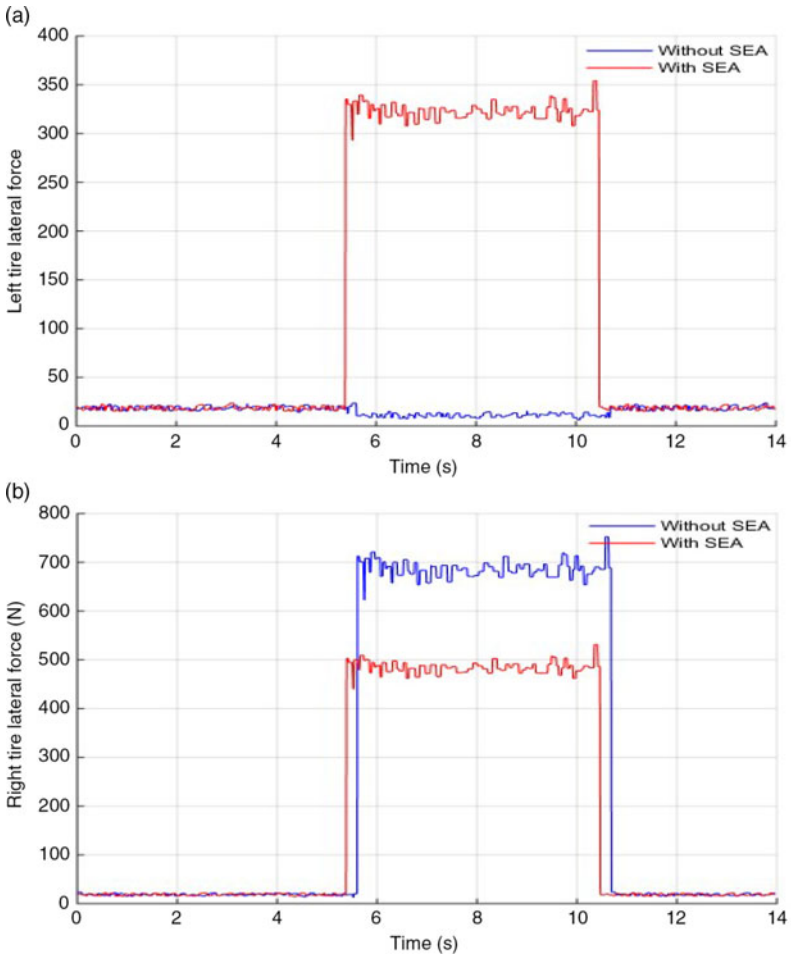


Fig. 13. Lateral force of the left and right ((a) left tire, (b) right tire).

https://doi.org/10.1017/S0263574720000156 Published online by Cambridge University Press

5.2. Experiment in rotational motion

Rotational motion of the Segway is tested on asphalt roads. The Segway is programmed to go straight and turn right, and then travel straight until the end of the experiment. The test-bed for rotational motion experiment is shown in Fig. 12.

The following two figures show the experimental results of the lateral force of the right and left tires with and without the SEA device (human weight is 80 kg, Segway weight is 35 kg, average speed of rotation is 2.1 m/s, and rotation radius is 0.6 m).

From the analysis of Fig. 13, we can see that when the Segway is traveling straight, the deflection angle is negligible, and lateral force is very small. At about 5.8 s, just at the moment of turning right, the center of gravity shifts, and almost all the pressure acts on the right tire, causing the lateral force to increase rapidly. The pressure on the left tire is very low, resulting in a very small lateral force. These conditions lead to uneven forces on the left and right tires. Without using the SEA force compensation device, the lateral forces of the left and right tires differ by about 668 N. After using the SEA force compensation device, the lateral forces of the left and right tires differ by about 162 N. Thus, we observe that the SEA can effectively reduce the instability of the body due to uneven forces on the left and right tires as well as the possibility of rollover. The lateral force acting on the left and right tire, difference of two tires, and compensated force in this experiment are summarized in Table III.

6. Conclusion

In this study, a design and control of the SEA to compensate for the external force (impact, vibration, centripetal force, etc.) on the tire has been proposed. Also, the SEA has been successfully incorporated into the Segway, and experiments were conducted to evaluate the compensation for the disturbances and centripetal force. When the Segway runs fast in a bumpy area, the longitudinal forces are adversely affected by impact and vibration. By controlling the SEA, the disturbances acting on these longitudinal forces can be reduced. Using the SEA, in this case, the average of compensation force is about 108 N (in Fig. 11 and Table II). In the turning motion, the lateral forces action on the two tires can be increased by the high centripetal force. If the difference in lateral forces acting on the left and right tires is large, the Segway can be easily rolled over. To reduce difference, the SEA has been utilized in this research. In this case, the average of compensation force to balance the lateral forces action on the two tires is about 506 N (in Fig. 13 and Table III). It is concluded that the SEA device can effectively improve driving comfort when driving on bumpy roads or on the curved path. However, there exists the large vibration at the bumpy area as shown in Fig. 11 and SEA system does not reduce the vibration in the uneven road. To reduce the vibration, the mechanical impedance of the SEA needs to be optimized, which is left as a future research work. In order to improve the stability of the Segway, also, it needs to find the solution for resolving disturbances using the vehicle dynamics, to estimate the friction coefficient in real time based on the force of the tire, and to optimize the controller.

Acknowledgments

This material is based upon work supported by the Ministry of Trade, Industry and Energy (MOTIE, Korea) under Industrial Technology Innovation Program. No. 10062443 “40 km/h of balancing robot with active suspension.”

References

1. J. W. Joh and G. T. Park, “Reasonable Hardware Design Methods for 2-Wheeled Mobile Robots: Based on Segway Type Mobile Robots,” *Proceedings of ICS2009-KIEE* (2009) pp. 109–111.
2. M. R. Bageant, “Balancing a Two-Wheeled Segway Robot,” *Bachelor’s Thesis* (Massachusetts Institute of Technology, 2011).
3. S. F. Kwak, M. H. Lee and B. J. Choi, “Design of fuzzy logic controller for inverted pendulum-type mobile robot,” *J. Daegu Gyeongbuk Stud.* **11**(3), 119–131 (2012).
4. J. H. Ra, J. H. Lim, S. H. Jeon and M. J. Chung, “Attitude Control of Segway Using PID Controller,” *Proceedings of KSME Spring Conference* (2015) pp. 3549–3552.
5. B. W. Kim, S. J. Hwang and B. S. Park, “A Low-Complexity Controller Design for Segway,” *Proceedings of KIEE Summer Conference* (2015) pp. 1339–1340.
6. S. J. Yoo, J. S. Jo, S. H. You and K. I. Lee, “A VDC Controller Design for Rollover Prevention and Lateral Stability Improvement of Vehicle,” *Proceedings of AUTO JOURNAL: Journal of the Korean Society of Automotive Engineers* (2006) pp. 766–775.

https://doi.org/10.1017/S0263574720000156 Published online by Cambridge University Press

7. K. M. Goher, M. O. Tokhi and N. H. Siddique, "Dynamic modeling and control of a two wheeled robotic vehicle with a virtual payload," *J. Eng. Appl. Sci.* **6**(3), 7–41 (2011).
8. A. Castro, Modeling and dynamic analysis of a two-wheeled inverted-pendulum, *M.S. Thesis* (Georgia Institute of Technology, 2012).
9. G. A. Pratt and M. M. Williamson, "Series Elastic Actuators," *Proceedings of IEEE/RSJ International Conference on Intelligent Robot Interaction and Cooperative Robots*, PA, USA (1995) pp. 388–406.
10. L. Liu, X. Wang, L. Jin and S. Shi, "Modeling and Analysis on Effect of Driving Force for Vehicle Stability," *Proceedings of 2011 International Conference on Transportation, Mechanical, and Electrical Engineering (TMEE)*, Changchun, China (2001) pp. 1228–1231.
11. T. Shim and D. Margolis, "An analytical tire model for vehicle simulation in normal driving conditions," *International Journal of Vehicle Design* **35**(3), 224–240 (2004).
12. E. Bakker, H. B. Pacejka, and L. Lidner, "A new tire model with an application in vehicle dynamics studies," *SAE Transactions* **98**(Section 6: JOURNAL OF PASSENGER CARS), 101–113 (1989).
13. H. B. Pacejka and E. Bakker, "The magic formula tyre model," *Veh. Syst. Dyn*. **21**(supplement) (1991).
14. E. Bakker, L. Nyborg and H. B. Pacejka, "Tyre modeling for use in vehicle dynamics studies," SAE Technical Paper Series (1987).
15. H. B. Pacejka, Tyre and Vehicle Dynamics (Butterworth-Heinemann, 2002).
16. P. Guaneri, G. Rocca and M. Gobbi, "A neural-network-based model for the dynamic simulation of the tire/suspension system while traversing road irregularities," *IEEE Trans. Neural Networks* **19**(9), 1549–1563 (2008).
17. L. Palkovics and M. El-Gindy, "Neural network representation of tyre characteristics: the neuro-tyre," *Int. J. Veh. Des.* **14**(5), 56325911 (1993).
18. G. Wang, *Recent Advances in Robotic Systems* (InTech, London, 2016).
19. S. Arumugom, S. Muthuraman and V. Ponselvan, "Modeling and application of series elastic actuators for force control multi legged robots," *J. Comput.* **1**(1), 26–33 (2009).
20. T. S. Tumapala, S. S. Saini, U. Sarker and D. D. Ray, "Compliance Control of Tele-Robot," *Proceedings of Conference on Advances in Robotics*, Mumbai, India (2013) pp. 1–7.
21. S. H. Oh and K. C. Kong, "High-precision robust force control of a series elastic actuator," *IEEE/ASME Trans. Mechatron.* **22**(1), 71–80 (2017).

https://doi.org/10.1017/S0263574720000156 Published online by Cambridge University Press